Effect of anomalous magnetic moment on the chiral transition at zero temperature in a strong magnetic field

Rui He and Xin-Jian Wen*

Institute of Theoretical Physics, State Key Laboratory of Quantum Optics and Quantum Optics Devices, Shanxi University, Taiyuan, Shanxi 030006, China

(Received 24 October 2022; accepted 5 December 2022; published 29 December 2022)

The effect of the anomalous magnetic moment (AMM) on the chiral restoration is investigated at zero temperature in the strong magnetic fields with the vacuum magnetic regularization scheme. It is shown that the chiral restoration diagram sensitively depends on the AMM in the ultrastrong magnetic fields. In our work, the parametrization of AMM is employed as proportional to the square of the chiral condensate. The critical chemical potential is found to decrease linearly by the increasing coefficient in the AMM scale. At a smaller scale of the AMM, the critical chemical potential could go down and then grow up as the magnetic field increases. But at a larger scale, the magnetic catalysis on the critical chemical potential would not happen anymore.

DOI: 10.1103/PhysRevD.106.116023

I. INTRODUCTION

Quantum chromodynamics (QCD) is a basic theory to study the strong interaction between quarks and gluons. It has two main striking features; asymptotic freedom and color confinement [1]. The study of the QCD phase diagram in the temperature-density plane is a topic that has attracted much attention over many years. Additionally, the QCD phase diagram also depends on external parameters, such as the presence of strong magnetic fields and high densities, which are interesting to investigate from both experimental and theoretical points of view. It is well known that, heavy ion collisions can produce a very strong magnetic field and the order of magnitude is up to about $eB \sim 10^{19}$ Gauss. In the astrophysical environment, strong magnetic fields still exist in the interior of magnetars [2,3]. In the peripheral collisions of nuclei, extremely larger magnetic field up to 10^{18} or higher value can be generated [4–6]. Theoretically, the maximum strengths of the order 10^{20} Gauss in the interior of stars are proposed by an application of the virial theorem [7,8], and even higher fields could be generated during the electroweak phase transition in the early Universe [9,10].

In recent studies, the chiral phase transition and the equation of state of dense matter were explored in the strong magnetic field [11–17]. Especially, it is known that the magnetic catalysis (MC) plays as an important phenomenon, where a magnetic field enhances the spontaneous chiral symmetry breakdown. The more general results state that a constant magnetic field leads to the generation of a fermion dynamical mass [18–20]. However, in the region close to the (pseudo) critical temperature, the inverse magnetic catalysis effect (IMC) is proposed by the lattice QCD result [21]. The finite background magnetic field leads to the breaking of the chiral symmetry and triggers the production of quark anomalous magnetic moments (AMM) [22,23]. In literature, the AMM is originally found in the weak-field region, and the Schwinger linear-in-B ansatz for the AMM of quarks is widely considered [24]. In the strong magnetic field region, the AMM from the one-loop fermion self-energy depends on the Landau level and decreases with it [25]. The fact of the dynamic generation of AMM is mainly suggested due to the lowest Landau level (LLL) effect [26]. Recently, a quark AMM proportional to the square of chiral condensate ($\kappa_u = \kappa_d = \upsilon\sigma^2$) was suggested to produce results of chiral condensate as functions of the temperature and the magnetic field in good agreement with the lattice result [27]. The AMM was expected to play an important role to induce the IMC effect around the critical temperature [17,28].

The Nambu-Jona-Lasinio (NJL) model was first proposed as a low energy effective theory for QCD to describe nucleons and mesons. It was successfully developed to investigate the QCD chiral symmetry and vacuum spontaneous breakdown at finite density and/or temperature in a strong magnetic field. However, the four-fermion interaction in the model leads to the nonrenormalization of the NJL model, so a proper regularization scheme is needed to avoid ultraviolet divergences. The familiar regularization

*wenxj@sxu.edu.cn

schemes are Pauli-Villars scheme [29–31], the vacuum magnetic regularization scheme (VMR) [32–34], the magnetic field independent regularization scheme (MFIR) [35], and non-MFIR scheme. Unfortunately, the non-MFIR schemes will produce nonphysical oscillation behavior in chiral quark condensate or tachyonic neutral pion masses [36]. The MFIR scheme and the VMR scheme are helpful to extract physical content from the vacuum of the strong interaction affected by a magnetic field. In this work, we will employ the VMR scheme to deal with the divergencies in the thermodynamic potential and discuss the influence of AMM on the chiral phase transition at finite densities. The effect of AMM on the chiral restoration at finite temperature has been studied by the VMR scheme with convincing results [34]. Our aim focuses on the possible AMM scale dependent on the chiral quark condensate and its effect on the critical chemical potential in a strong magnetic field.

The paper is organized as follows. In Sec. II, we present the thermodynamics of the two-flavor NJL model with nonzero AMM in a strong magnetic field. In Sec. III, the numerical results are shown with a detailed investigation on the influence of AMM on chiral phase transition. The last section is a short summary.

II. THERMODYNAMICS OF THE SU(2) NJL MODEL AT ZERO TEMPERATURE

In the SU(2) version of the NJL model under a strong magnetic field, the Lagrangian density of the two-flavor NJL model is given by

$$\mathcal{L}_{\mathrm{NJL}} = \bar{\psi}\left(i\not{D} - m + \frac{1}{2}\hat{a}\sigma^{\mu\nu}F_{\mu\nu}\right)\psi + G[(\bar{\psi}\psi)^2 + (\bar{\psi}i\gamma_5\vec{\tau}\psi)^2], \tag{1}$$

where ψ represents a flavor isodoublet (u and d quarks) and $\vec{\tau}$ is the isospin Pauli matrix. The coupling of the quarks to the electromagnetic field is introduced by the covariant derivative $\not{D} \sim \gamma^\mu D_\mu$ and $D_\mu = \partial_\mu - ie\hat{Q}A_\mu$. The charge matrix is given by $\hat{Q} \equiv \mathrm{diag}(q_u, q_d) = \mathrm{diag}(2/3, -1/3)$. The Abelian gauge field A_μ stands for the external magnetic field B aligned along the z-direction. The AMM is introduced by the $\sigma^{\mu\nu} = i[\gamma^\mu, \gamma^\nu]/2$ coupling with electromagnetic field strength $F^{\mu\nu} = \partial^\mu A^\nu - \partial^\nu A^\mu$. The matrix tensor used in this work is $g^{\mu\nu} = \mathrm{diag}(1, -1, -1, -1)$. The factor $\hat{a} = \hat{Q}\hat{\kappa}$, where $\hat{\kappa} = \mathrm{diag}(\kappa_u, \kappa_d)$, is a 2×2 matrix in the flavor space; here κ_i are AMM of the quarks, The more recent results suggested that the proper form of AMM would change with the chiral condensate, since it involves the behavior related to the condensate [27].

By expanding $\bar{\psi}\psi$ around the quark condensate $\langle\bar{\psi}\psi\rangle$ and dropping the quadratic term of the fluctuation, one can get the mean-field approximation $(\bar{\psi}\psi)^2 \approx 2\langle\bar{\psi}\psi\rangle(\bar{\psi}\psi) - \langle\bar{\psi}\psi\rangle^2$. The dynamical quark mass is given by

$$M_i = m - 2G\langle\bar{\psi}\psi\rangle, \tag{2}$$

where the quark condensates include u and d quark contributions as $\langle\bar{\psi}\psi\rangle \equiv \sigma = \sum_{i=u,d}\sigma_i$. The dynamical mass depends on both flavors condensates. Therefore, the same mass $M_u = M_d = M$ is available for u and d quarks. The contribution from the i flavor quark is [34]

$$\sigma_i = \sigma_i^{\mathrm{vac}} + \sigma_i^{\mathrm{field}} + \sigma_i^{\mathrm{mag}} + \sigma_i^{\mathrm{med}}. \tag{3}$$

The terms σ_i^{vac}, $\sigma_i^{\mathrm{field}}$, and σ_i^{mag} represent the vacuum, the field, and the magnetic field to the quark condensation, respectively. The regularized vacuum contribution reads

$$\sigma_i^{\mathrm{vac}} = -\frac{MN_c}{2\pi^2}\left\{\Lambda\epsilon_i(\Lambda) - K_{0i}^2\ln\left[\frac{\Lambda + \epsilon_i(\Lambda)}{K_{0i}}\right]\right\}, \tag{4}$$

where a 3D sharp cutoff Λ of the momentum is employed. The definitions $K_{0i} = \sqrt{M^2 + \kappa_i^2 B_i^2}$ and $\epsilon_i^2(\Lambda) = K_{0i}^2 + \Lambda^2$ are adopted to include the AMM with the parameter B_i defined as $B_i = q_i eB$ [34]. The finite magnetic field-dependent contributions are given by

$$\sigma_i^{\mathrm{field}} = -\frac{MN_c B_i^2}{24\pi^2}\frac{[3(\alpha_i+1)^2 - 1]}{K_{0i}^2}, \tag{5}$$

$$\sigma_i^{\mathrm{mag}} = -\frac{MN_c}{4\pi^2}\int_0^\infty \frac{ds}{s^2}e^{-sK_{0i}^2} \times \left\{\frac{B_i s\cosh[(\alpha_i+1)B_i s]}{\sinh(B_i s)} - 1 - \frac{1}{6}[3(\alpha_i+1)^2 - 1](B_i s)^2\right\} \tag{6}$$

with the notation $\alpha_i = 2M\kappa_i$. σ_i^{med} is contribution of medium at zero temperature, given by the following expression

$$\sigma_i^{\mathrm{med}} = \frac{MN_c|B_i|}{2\pi^2}\sum_{n=0}^{n_{\max}}\sum_{s=\pm1}\left(1 - \frac{sT_i}{M_{\mathrm{nis}}}\right)\ln\left(\frac{\mu_i + p_F}{M_{\mathrm{nis}} - sT_i}\right), \tag{7}$$

where we have adopted the Landau-level induced energy eigenvalue

$$M_{\mathrm{nis}} = \sqrt{\left(2n + 1 - s\frac{q_i}{|q_i|}\right)|B_i| + M^2}, \tag{8}$$

and the longitudinal Fermi momentum

$$p_F = \sqrt{\mu_i^2 - \left(\sqrt{\left(2n + 1 - s\frac{q_i}{|q_i|}\right)|B_i| + M^2} - sT_i\right)^2}, \tag{9}$$

Due to the requirement $p_F \geq 0$, one can get the maximum Landau-level number

$$n_{\max} = \mathrm{Floor}\left[\frac{1}{2}\left(\frac{(sT_i+\mu_i)^2 - M^2}{|B_i|} + s\frac{q_i}{|q_i|} - 1\right)\right], \quad (10)$$

where $T_i = \kappa_i B_i$ includes the AMM according to the Schwinger linear ansatz [26], and $s = \pm 1$ stands for the spin of the quark. The AMM separates the energies of the up and down spins in the LLs ($n \neq 0$), in addition to the LLL ($n = 0$).

In the VMR scheme, the NJL thermodynamic potential density can be written as [34]

$$\Omega_i = \frac{(M-m)^2}{4G} + \sum_{i=u,d} \Omega_i^{\mathrm{vac}} + \Omega_i^{\mathrm{field}} + \Omega_i^{\mathrm{mag}} + \Omega_i^{\mathrm{med}}. \quad (11)$$

The contributions Ω_i^{vac} and $\Omega_i^{\mathrm{field}}$ must be regularized and the following expressions are given by

$$\Omega_i^{\mathrm{vac}} = -\frac{N_c}{8\pi^2}\left\{\Lambda[\Lambda^2 + \epsilon_i^2(\Lambda)]\epsilon_i(\Lambda) - K_{0i}^4 \ln\left[\frac{\Lambda + \epsilon_i(\Lambda)}{K_{0i}}\right]\right\}, \quad (12)$$

$$\Omega_i^{\mathrm{field}} = -\frac{N_c B_i^2}{48\pi^2}[3(\alpha_i+1)^2 - 1]\ln\frac{K_{0i}^2}{\Lambda^2}, \quad (13)$$

Because of the ultraviolet divergence, we still use the 3D sharp cutoff scheme to regularize the vacuum term. The Ω_i^{mag} is the magnetic field contributions [34],

$$\Omega_i^{\mathrm{mag}} = \frac{N_c}{8\pi^2}\int_0^\infty \frac{ds}{s^3} e^{-sK_{0i}^2}\left\{\frac{B_i s\cosh[(\alpha_i+1)B_i s]}{\sinh(B_i s)} - 1 - \frac{1}{6}[3(\alpha_i+1)^2 - 1](B_i s)^2\right\}. \quad (14)$$

The contribution of the medium at zero temperature Ω_i^{med} is

$$\Omega_i^{\mathrm{med}} = -\frac{N_c|B_i|}{4\pi^2}\sum_{n=0}^{n_{\max}}\sum_{s=\pm 1}\left[p_F\mu_i - (M_{\mathrm{nis}} - sT_i)^2 \times \ln\left(\frac{\mu_i + p_F}{M_{\mathrm{nis}} - sT_i}\right)\right]. \quad (15)$$

From the thermodynamic potential, the quark number density is easily evaluated as follows:

$$\rho_i = \frac{N_c|B_i|}{2\pi^2}\sum_{n=0}^{n_{\max}}\sum_{s=\pm}\sqrt{\mu_i^2 - (M_{\mathrm{nis}} - sT_i)^2}. \quad (16)$$

For completeness, at the zero AMM, the replacements of $K_{0i} \to M$, $\alpha_i \to 0$, and $T_i \to 0$ should be done in Eqs. (4)–(7) to get the gap equation. It has been verified that the thermodynamic potential Ω_{VMR} can be taken as a modification of the potential Ω_{MFIR} by an additional term, which is independent on the effective mass M [32]. As a consequence, the gap equation in VMR scheme is compatible with the result from MFIR scheme in Ref. [37]. Specially, the vacuum effective mass M without AMM is still given by

$$\frac{M-m}{2G} = -\frac{MN_cN_f}{2\pi^2}\left\{\Lambda\epsilon_i(\Lambda) - M^2\ln\left[\frac{\Lambda+\epsilon_i(\Lambda)}{M}\right]\right\} + \sum_{i=u,d}\frac{MN_c|B_i|}{2\pi^2}\left\{\ln[\Gamma(x_i)] - \frac{1}{2}\ln(2\pi) + x_i - \frac{1}{2}(2x_i-1)\ln(x_i)\right\}, \quad (17)$$

where $x_i = M^2/|2B_i|$ is defined [37]. The detailed derivation of the equivalence of the gap equations in two schemes can be found in Ref. [32].

III. NUMERICAL RESULT AND DISCUSSION

In this section, the AMM effect at high densities is studied in terms of the chiral phase transition in the strong magnetic field. In the present calculation, the following parameters are adopted; $m_u = m_d = 4.548$ MeV, $\Lambda = 719.23$ MeV, and $G = 1.954/\Lambda^2$. In Ref. [27], the three forms of the AMM ($\kappa =$ constant, $\kappa = \upsilon\sigma$, and $\kappa = \upsilon\sigma^2$) were compared and discussed. The scale proportional to the square of the condensate was considered as the practicable effective form to describe the thermomagnetic properties of QCD. The AMMs for u and d quarks in our work are adopted as $\kappa_u = \kappa_d = \upsilon\sigma^2$. The opposite signs $\kappa_u = -\kappa_d = \upsilon\sigma^2$ for possible negative contribution of d quarks are considered for comparison. The quark dynamical mass as a function of the chemical potential in different magnetic fields can be obtained by solving the gap equation Eq. (2), Then we can analyze the effect of AMM on the critical chemical potential for the first-order phase transition. In the calculations, we assume the isospin symmetric case meaning that the chemical potentials are equal $\mu_u = \mu_d = \mu$ for u and d quarks.

In Fig. 1, the vacuum mass is shown as a function of the magnetic field intensity. The three AMMs $\kappa = 0$, $\kappa_u = \kappa_d = 0.9\sigma^2$, and $\kappa_u = -\kappa_d = 0.9\sigma^2$ are marked by the black solid, the red dotted, and the blue dashed lines respectively. The behavior of the effective quark mass enhanced by the magnetic field is consistent with the result pointed in Ref. [37]. From the figure, it is clearly seen that the growing behavior of the effective mass is relatively slightly enhanced by the nonzero AMM, where the larger magnitude of the magnetic field facilitates the binding of the quark and antiquark.

In Fig. 2 we show the dynamical quark effective mass as functions of the chemical potential at the different AMMs in four panels. The magnetic fields are adopted from 0.1 GeV^2 to 0.5 GeV^2, which are clearly marked by the curves from bottom to top in the vacuum state.

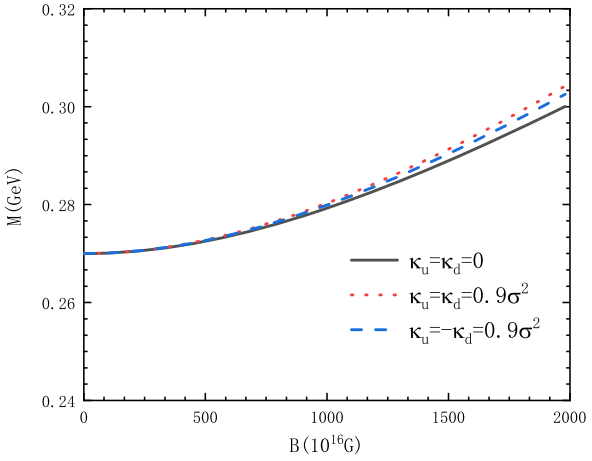

FIG. 1. The behavior of the effective quark mass in vacuum state with and without AMMs as a function of the magnetic field.

The descending behavior of quark mass occurs in the chiral restoration process, which is not a smooth slope but a sudden drop denoting the first-order transition. In the magnetic field of 0.2 GeV^2 or even higher order, the quarks only occupy the LLL to give rise to a single first-order phase transition. For the weaker magnetic field $eB = 0.1$ GeV^2 marked by the solid lines, the maximum Landau levels for u and d quarks are mismatched [38]. In Table I, the quantum number of maximum Landau levels $n_{u,\max}$ and $n_{d,\max}$ is listed in the chemical potential μ range from vacuum to the chiral restoration. At $\mu > 267$ MeV for $\kappa = 0$ or $\mu > 263$ MeV for $\kappa = 0.5\sigma^2$, the LLL ($n = 0$) occurs for u- and d-quarks. When the chemical potential increases up to about 302 MeV, the energy level is excited to a higher level for d quarks, while the u quarks still lie in the LLL. The quarks occupation would influence the

TABLE I. The quantum number of Landau Levels occupied by quarks for the magnetic field $eB = 0.1$ GeV^2 at different AMMs. The number "0" means the LLL.

AMM (κ/σ^2)	μ (MeV)	$n_{u,\max}$	$n_{d,\max}$
0	$0 \sim 267$	No	No
	$267 \sim 303$	0	0
	$303 \sim 369$	0	1
0.5	$0 \sim 263$	No	No
	$263 \sim 302$	0	0
	$302 \sim 369$	0	1

condensate of quark and antiquarks. As a consequence, there are two first-order transitions in the region of densities. Comparing the panels (a) (b), and (d) in Fig. 2, it can be found that the AMM would result in the critical chemical potential moving to larger value with the increasing magnetic field in the region of $eB > 0.2$ GeV^2. It is characterized by the so-called MC effect and is compatible to the conclusion in the absence of AMM [38,39]. On the contrary in panel (c) in Fig. 2, the larger coefficient with the same sign of κ_u and κ_d would always produce the IMC effect, which is characterized by the decrease of the critical chemical potential as the magnetic field increases. By comparing the vertical axis on four panels, it can be found that the AMM has poor impact on the vacuum mass of quarks in the weak magnetic field. When the magnetic field becomes strong enough, the enhancement of the vacuum chiral condensate by the AMM becomes more evident. The effect of AMM is agreement with those obtained at finite temperature in Ref. [34]. It is concluded that the scale and sign of AMM would have significant effect on the realization of the MC and IMC.

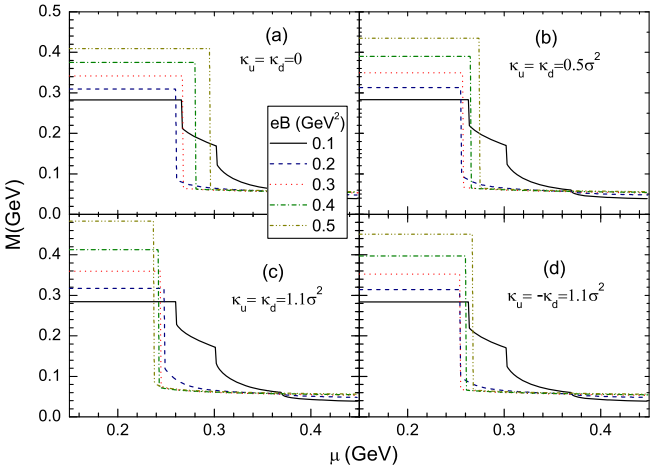

FIG. 2. The quark effective mass as a function of chemical potentials for different magnetic fields at the AMMs (a) $\kappa_u = \kappa_d = 0$, (b) $\kappa_u = \kappa_d = 0.5\sigma^2$, (c) $\kappa_u = \kappa_d = 1.1\sigma^2$, and (d) $\kappa_u = -\kappa_d = 1.1\sigma^2$.

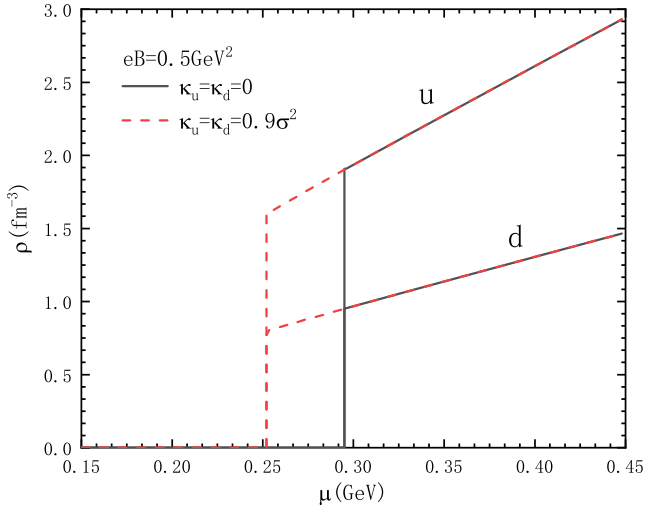

FIG. 3. The quark number density with and without AMMs as a function of the chemical potential.

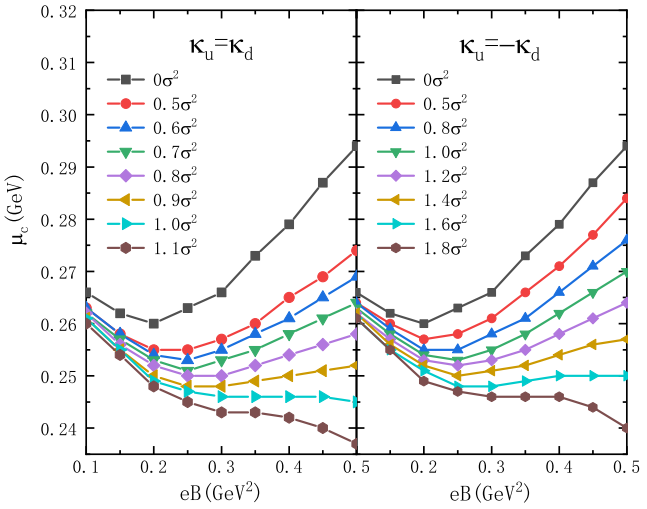

FIG. 4. The behavior of the critical chemical potential for different AMM scales as a function of the magnetic field.

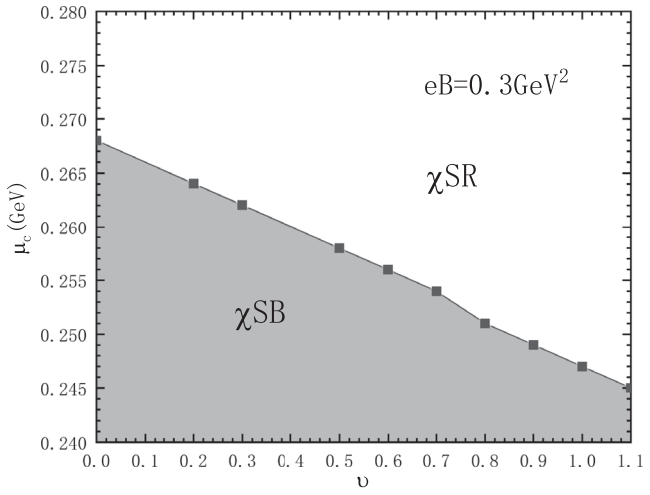

FIG. 5. The critical chemical potential as a function of the coefficient υ and the region of χSR and χSB is separated for the magnetic field $eB = 0.3$ GeV^2.

In the strong magnetic field, the charged quark would be restricted in the Landau levels. The u and d quarks will have different densities with the same chemical potential due to their different electric chargers. In Fig. 3, the quark density ρ_u and ρ_d are shown at the magnetic field $eB = 0.5$ GeV^2. The presence of the AMM marked by the dashed lines affects not the number density but the position of the occurrence of quarks. The degenerate factor proportional to $|q_i B|$ is responsible for the relation $\rho_u > \rho_d$, where the absolute value of the electric charge of u quarks is larger than that of d quarks.

In Fig. 4, the critical chemical potential for the chiral restoration is shown as a function of the magnetic field at the AMMs: $\kappa_u = \kappa_d$ on left panel and $\kappa_u = -\kappa_d$ on right panel. The different coefficients of the AMM proportional to the square of the chiral condensate are marked on the lines. For the $\kappa_u = \kappa_d < 1.0\sigma^2$ on left panel, one would see the behavior of the critical chemical potential μ_c going down and up with the increase of the magnetic field. On these nonmonotonously curves, there exists a special value for the magnetic field eB_c, above which the MC effect is revealed by the increase of μ_c with the increase of eB. While for the magnetic fields below the value, the IMC effect would operate slightly in a short range. But as the coefficient of AMM increases up to 1.0, the nonmonotonous behavior disappears and the IMC effect would be always realized in the whole range of the magnetic field. If the sign of the AMM for u and d quarks is opposite, namely, $\kappa_u = -\kappa_d = \upsilon\sigma^2$, a similar behavior of μ_c is obtained in addition to that the much larger coefficient is available at the same μ_c on right panel. Generally speaking, for two cases at any fixed magnetic field, it can be concluded that the larger coefficient of AMM would lead to the smaller μ_c for the chiral transition.

In Fig. 5, the critical chemical potential μ_c is shown as a function of the coefficient of AMM at the magnetic field $eB = 0.3$ GeV^2. It is interestingly found that the μ_c is nearly a linearly decreasing function of the coefficient of AMM. The gray part below the critical line denotes the chiral symmetry breaking (χSB). At the chemical potential larger than μ_c, the chiral symmetry restoration (χSR) is expected to take place in the upper blank region. The AMM with the coefficient larger than 1.0 will result in a decrease of μ_c close to 10% of the original value without AMM.

The scale of AMM could have a significant impact on the role of the magnetic field in the chiral restoration. As was discussed above, there is a critical magnetic field separating the region of MC and IMC discovered in Fig. 4. Now one can continuously change the coefficient of AMM proportional to the square of chiral condensate and get the whole diagram of MC and IMC in the eB-υ plane in Fig. 6.

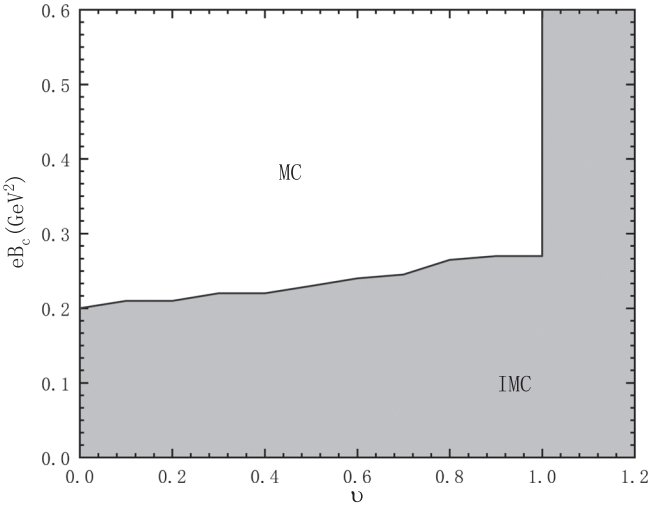

FIG. 6. The regions of MC and IMC are shown in the eB-υ plane.

The boundary between the MC and IMC is described by a solid line. For a given scale of the AMM, the IMC effect can always be realized in a weaker magnetic field marked by the gray area and the MC effect in a stronger magnetic field marked by the empty region. But for the coefficient of the AMM increasing up to 1.0, the larger value of the AMM $\kappa = 1.0\sigma^2$ is obtained and the IMC region would expand to the whole area. On the other hand, for a given magnetic field, the increase of the coefficient of the AMM could make the possibility for the MC turning to the IMC effect. It can be concluded that the scale of AMM is crucial to account for the happening of IMC and MC effects in the chiral restoration.

IV. SUMMARY

In this paper, we have explored the effect of the AMM on the chiral restoration at zero temperature to the strong magnetic fields. The VMR scheme has been used to avoid UV divergence. The chiral restoration happens with a sudden drop to indicate a first-order transition at larger densities. We found that the AMM proportional to the square of the chiral condensate, i.e., $\kappa = \upsilon\sigma^2$, has a crucial impact on the chiral restoration. Even though the effect of the AMM can be negligible in the region of the weak magnetic field, the enhancement of the dynamical vacuum mass is very sensitive to the AMM as the magnetic field becomes stronger. The critical chemical potential would slightly decrease with the increasing coefficient in the scale of the AMM $\kappa = \upsilon\sigma^2$. The AMM of $\kappa > 1.0\sigma^2$ would give rise to a decrease of the critical chemical potential up to 10% of the original value without AMM.

In the case of small scale of AMM, the critical chemical potential is a nonmonotonous function of the magnetic field. In the convex behavior, it is seen that the IMC effect occurs in weaker magnetic fields and the MC effect occurs in stronger magnetic fields. The increase of the coefficient υ would turn the MC effect into IMC effect. For the larger scale near to $\kappa = 1.0\sigma^2$, the inverse magnetic catalysis region would expand to the whole area in the eB-υ plane. So it is concluded that the occurrence of the MC effect, namely, the decrease of the critical chemical potential with the magnetic field, would constrain an upper limit on the scale of the AMM. It is expected that our result is instructive for the investigation on AMM in future experiments.

ACKNOWLEDGMENTS

The authors would like to thank support from the National Natural Science Foundation of China under the Grants No. 11875181, No. 11705163, and No. 12147215. This work was also sponsored by the Fund for Shanxi "1331 Project" Key Subjects Construction.

[1] D. J. Gross and F. Wilczek, Phys. Rev. D **8**, 3633 (1973).
[2] R. C. Duncan and C. Thompson, Astrophys. J. Lett. **392**, L9 (1992).
[3] C. Thompson and R. C. Duncan, Astrophys. J. **408**, 194 (1993).
[4] V. Voronyuk, V. D. Toneev, W. Cassing, E. L. Bratkovskaya, V. P. Konchakovski, and S. A. Voloshin, Phys. Rev. C **83**, 054911 (2011).
[5] A. Bzdak and V. Skokov, Phys. Lett. B **710**, 171 (2012).
[6] W. T. Deng and X. G. Huang, Phys. Rev. C **85**, 044907 (2012).
[7] D. E. Kharzeev, L. D. McLerran, and H. J. Warringa, Nucl. Phys. **A803**, 227 (2008).
[8] V. Skokov, A. Y. Illarionov, and V. Toneev, Int. J. Mod. Phys. A **24**, 5925 (2009).
[9] L. Campanelli, Phys. Rev. Lett. **111**, 061301 (2013).
[10] T. Vachaspati, Phys. Lett. B **265**, 258 (1991).
[11] D. Lai, Rev. Mod. Phys. **73**, 629 (2001).
[12] V. A. Miransky and I. A. Shovkovy, Phys. Rep. **576**, 1 (2015).
[13] E. J. Ferrer, V. de la Incera, and P. Sanson, Phys. Rev. D **103**, 123013 (2021).
[14] X. J. Wen, S. Z. Su, D. H. Yang, and G. X. Peng, Phys. Rev. D **86**, 034006 (2012).
[15] X. J. Wen, Phys. Rev. D **88**, 034031 (2013).
[16] D. P. Menezes, M. B. Pinto, and C. Providência, Phys. Rev. C **91**, 065205 (2015).
[17] X. J. Wen, R. He, and J. B. Liu, Phys. Rev. D **103**, 094020 (2021).
[18] V. P. Gusynin, V. A. Miransky, and I. A. Shovkovy, Phys. Rev. Lett. **73**, 3499 (1994); **76**, 1005(E) (1996).
[19] V. P. Gusynin, V. A. Miransky, and I. A. Shovkovy, Phys. Lett. B **349**, 477 (1995).
[20] V. A. Miransky and I. A. Shovkovy, Phys. Rev. D **66**, 045006 (2002).
[21] M. D'Elia and F. Negro, Phys. Rev. D **83**, 114028 (2011).
[22] L. Chang, Y. X. Liu, and C. D. Roberts, Phys. Rev. Lett. **106**, 072001 (2011).
[23] Pedro J. de A. Bicudo, J. E. Ribeiro, and R. Fernandes, Phys. Rev. C **59**, 1107 (1999).
[24] S. Fayazbakhsh and N. Sadooghi, Phys. Rev. D **90**, 105030 (2014).
[25] E. J. Ferrer, V. de la Incera, D. Manreza Paret, A. Pérez Martínez, and A. Sanchez, Phys. Rev. D **91**, 085041 (2015).
[26] J. S. Schwinger, Phys. Rev. **73**, 416 (1948).
[27] M. Kawaguchi and M. Huang, arXiv:2205.08169.
[28] K. Xu, J. Chao, and M. Huang, Phys. Rev. D **103**, 076015 (2021).
[29] S. Mao, Phys. Rev. D **99**, 056005 (2019).
[30] S. Mao, Phys. Lett. B **758**, 195 (2016).

[31] N. Chaudhuri, S. Ghosh, S. Sarkar, and P. Roy, Phys. Rev. D **103**, 096021 (2021).
[32] S. S. Avancini, R. L. S. Farias, M. B. Pinto, T. E. Restrepo, and W. R. Tavares, Phys. Rev. D **103**, 056009 (2021).
[33] W. R. Tavares, R. L. S. Farias, S. S. Avancini, V. S. Timóteo, M. B. Pinto, and G. Krein, Eur. Phys. J. A **57**, 278 (2021).
[34] R. L. S. Farias, W. R. Tavares, R. M. Nunes, and S. S. Avancini, Eur. Phys. J. C **82**, 674 (2022).
[35] R. M. Aguirre, Phys. Rev. D **102**, 096025 (2020).
[36] N. Chaudhuri, S. Ghosh, S. Sarkar, and P. Roy, Phys. Rev. D **99**, 116025 (2019).
[37] D. P. Menezes, M. B Pinto, S. S. Avancini, A. P. Martinez, and C. Providencia, Phys. Rev. C **79**, 035807 (2009).
[38] Y. Wang and X. J. Wen, Phys. Rev. D **105**, 074034 (2022).
[39] A. F. Garcia and M. B. Pinto, Phys. Rev. C **88**, 025207 (2013).